Memorias del 2024 Congreso Nacional de Control Automático
8-11 de Octubre, 2024. Ciudad de México, México.

Multifault observer based detection method for Brushless DC motors

Alejandra de la Guerra * **Alejandro Gutiérrez-Giles** **

* *Universidad de las Américas Puebla, Ex-Hacienda Santa Catarina Mártir, 72810, San Andrés Cholula, Puebla, México (e-mail:alejandra.delaguerra@udlap.mx)*
** *Instituto Nacional de Astrofísica, Óptica y Electrónica, Luis Enrique Erro 1, San Andrés Cholula, Puebla, México (e-mail:alejandro.giles@inaoe.mx)*

Abstract: A detection and identification method for high resistance connection faults and open phase fault in Brushless DC motors is presented. The method uses the current and speed residuals to detect the type of fault, the faulty phase and the severity of the fault in the case of high resistance connection. The residuals are made by comparing the measured signals and their estimates. These estimates are obtained with an observer which reconstructs the stator currents using only the rotor position signal. An observability analysis is included to show that it is possible to reconstruct the currents from the position measurement. Numerical simulations are presented to validate the proposed fault detection scheme.

Keywords: Observers, fault detection, BLDC motor.

1. INTRODUCTION

The stator faults in an electric motor, shown in Figure 1, can be classified as: 1) Open phase faults, 2) short circuit faults (turn-to-turn, phase-to-phase or coil-to-coil) and 3) high resistance connection (HRC) (Kudelina et al., 2020).

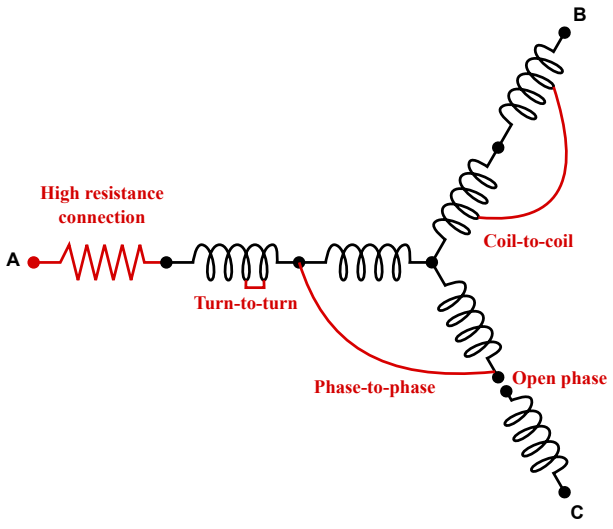

Fig. 1. Stator faults in a star connected BLDC motor

A high resistance connection is a fault caused by damage in the insulation of electrical connections or in the motor windings. It originates by poor soldering work, aging, corrosion, etc. This fault can be overlooked at its incipient state but if the contact resistance reaches a high level, the heat could brake open the insulation which could lead to open circuit faults (Wang et al., 2022). Therefore, these two faults are related and the open phase fault can occur after a HRC fault. This fault has been already studied for the induction motor, as in the work by Yun et al. (2009) among many other authors, but very few works, which are going to be discussed later on in this introduction, has been designed for BLDC trapezoidal motors.

HRC fault is modeled by adding a resistance in one of the stator phases to represent the asymmetry caused by this fault in the stator phases. Because it causes an imbalance in the stator currents, its effects can be perceived in the speed and torque signals. In this sense, the article by Gupta et al. (2021) presents an analysis of this fault using a dynamical model of the Brushless DC motor (BLDC), assuming: 1) that only permanent magnet is responsible of back emf in the stator windings, 2) there is not magnetic saturation. The author's conclusion was that HRC fault creates an asymmetry in the currents which leads to speed and torque ripples, it also mentions that the phase voltage is not significantly altered by this fault. Moreover, the fundamental frequency of the faulty current reduces and the torque signal presents a 2^{nd}, 4^{th} and 6^{th} harmonic under HRC fault.

HRC fault has been commonly detected using voltage drop measurement or infrared thermography (Yun et al.,

https://doi.org/10.58571/CNCA.AMCA.2024.056

2009). The drop measurement is made by a human operator with a voltmeter where the voltage drop is measure between the voltage source and the motor terminals. Therefore, this technique is inexpensive but it can be unreliable. The infrared thermography measures the temperature distribution using a thermal imaging camera to search for hot spots in the motor control system. This technique is highly reliable but expensive. Consequently, develop a reliable and cost-effective fault diagnosis and detection methods for the HRC fault is necessary.

Regarding HRC detection, the work by Wang et al. (2022) proposes a two-step method, where it is assumed that: 1) there is not magnetic saturation, 2) there are not other faults in the motor and 3) a balanced resistance network is connected in parallel with the motor to avoid influence from the inverter. The detection stage uses the spectrum of the Zero Sequence Voltage Component (ZSVC) to extract a fault indicator. It is shown that under HRC fault the voltage spectrum includes the faulty phase fundamental frequency component. On the other hand, the identification stage uses the ZSVC along with the current signals. It is shown that under fault, the ZSVC and the current signal have a synchronous trip which is used to construct an indicator. When a HRC fault occurs the indicator is less than zero for the faulty phase. The fault degree is obtained by calculating the magnitude of the voltage fundamental component. However, these results where obtained assuming that it is possible to access to the neutral point. Also, additional circuitry is necessary to guarantee that only permanent magnet is responsible of back emf, i.e., isolation from the inverter is assumed. Finally, the analysis is only useful for star connected BLDC motors.

Another method is presented in Gupta et al. (2024) where an input current based method is proposed. In the mentioned work it is assumed that: 1) six step control is used and therefore 2) Hall effect sensors are used for position measurement. First, it is shown that the input current can be used to detect HRC fault. Second, two condition indicators, variance and range of the input current along with a current moving window, are used to detect the fault. Next, additional information of the Hall effect sensors is used to indicate the faulty phase. Therefore, if the input current is already measured, not additional sensors are needed. Moreover, this method can be used for delta and star connected BLDC motors.

In this work, a model-based method is proposed to detect the HRC fault in a reliable manner, while indicating the severity of the fault by using the commonly available sensors. The scheme proposed is an observer based one, where the fault firms are obtained by proposing current and speed residuals. These residuals are the comparison between the measured and the estimated variables. Some of the highlights of this fault detection method are:

- It uses the already installed sensors i.e., encoder and stator current sensors.
- Also, it can detect an open stator phase fault and a HRC fault using the same residuals.
- It is shown that the current residual of the faulty phase increases as the HRC resistance increases, therefore this method can indicate the severity of the HRC fault.
- Moreover, this method can be implemented online using an integration moving window.

The paper is organized as follows, Section 2 recalls the mathematical model of the BLDC motor. Section 3 presents an observability analysis to found out if it is possible to reconstruct the stator phase currents using only the rotor position measurement. Section 4 presents the observer design and the proposed fault detection method. Section 5 shows the method validation via simulations. Finally, Section 6 includes the conclusions of this work.

2. PRELIMINARIES

2.1 Brushless DC motor mathematical model

In a BLDC motor, with Y-configuration, the windings are connected to a central point and power is applied to the remaining end of each winding. This means that the stator windings phases are balanced, which implies that the stator currents satisfy the following expression

$$i_1 + i_2 + ... + i_m = 0\,, \tag{1}$$

with m the number of stator phases. The motor has N_s stator slots and N_p rotor poles. It is assumed that stator windings are identical, i.e. the resistance and inductance parameters are the same for each phase.

The mathematical model of a balanced m-phases brushless DC motor as described by Chiasson (2005) is

$$\boldsymbol{D}\frac{d\boldsymbol{i}}{dt} = k_{\mathrm{e}}\omega\boldsymbol{E}(\theta) - \boldsymbol{R}\boldsymbol{i} + \boldsymbol{u} \tag{2a}$$

$$\frac{d\theta}{dt} = \omega \tag{2b}$$

$$J\frac{d\omega}{dt} = -k_{\mathrm{m}}\boldsymbol{E}^T(\theta)\boldsymbol{i} + \tau_{\mathrm{p}}(t) \tag{2c}$$

where $\boldsymbol{i} \in \mathbb{R}^m$ is the vector of stator currents, $\boldsymbol{u} \in \mathbb{R}^m$ is the vector of voltage inputs, $\omega \in \mathbb{R}$ is the angular velocity, $k_{\mathrm{e}} \in \mathbb{R}$ the back electromotive force constant, $k_{\mathrm{m}} \in \mathbb{R}$ the torque constant, $\boldsymbol{R} \in \mathbb{R}^{m\times m}$ is a diagonal matrix accounting for the winding resistances where the stator resistance is r, $\tau_{\mathrm{p}}(t) \in \mathbb{R}$ is the load torque, $J \in \mathbb{R}$ is the rotor inertia, and $\boldsymbol{D} \in \mathbb{R}^{3\times 3}$ is the inductance matrix is defined as

$$\boldsymbol{D} = \begin{bmatrix} \mathrm{L}+\mathrm{M} & 0 & 0 \\ 0 & \mathrm{L}+\mathrm{M} & 0 \\ 0 & 0 & \mathrm{L}+\mathrm{M} \end{bmatrix}, \tag{3}$$

with $\mathrm{L} \in \mathbb{R}$ the stator phase inductance an $\mathrm{M} \in \mathbb{R}$ the mutual inductance between stator phases. With this matrix definition it is implied that the phase currents are *balanced*.

On the other hand, the back–electromotive force vector is defined as

$$\boldsymbol{E} = \begin{bmatrix} e\left(\theta\right) \\ e\left(\theta - \dfrac{2\pi}{3}\right) \\ e\left(\theta - \dfrac{4\pi}{3}\right) \end{bmatrix}, \tag{4}$$

with $e(\theta)$ given by

$$e(\theta) = \begin{cases} \dfrac{6\theta}{\pi} & \text{if} -\pi/6 \leq \theta \leq \pi/6 \\ 1 & \text{if} \quad \pi/6 \leq \theta \leq 5\pi/6 \\ \dfrac{-6(\theta-\pi)}{\pi} & \text{if} \quad 5\pi/6 \leq \theta \leq 7\pi/6 \\ -1 & \text{if} \quad 7\pi/6 \leq \theta \leq 11\pi/6 \end{cases}, \tag{5}$$

where $e\left(\theta - \dfrac{2\pi}{3}\right)$ and $e\left(\theta - \dfrac{4\pi}{3}\right)$ are defined using (5) with the respective phase displacement.

3. OBSERVABILITY ANALYSIS

For the model (2a)-(2c), the first question to arise when designing an observer for either estimation or fault detection is if the states are observable given some measurable outputs. In this work, a fault detection approach is proposed based on the continuous generation of residual terms resulting from comparing model-based estimation currents with those measured directly and filtered by a low-pass filter. The following observability analysis will be carried out with the following considerations: 1) only rotor position is measured and 2) the load torque τ_{p} is zero. This simplification is made since τ_{p} is not a control input and thus if the simplified system is not observable, we cannot make the complete system observable by manipulating it. Due to the nonlinear nature of the model, we will employ nonlinear observability tools in order to obtain (hopefully) a global result. Let us construct the observation space $\mathcal{O}$ as follows(Isidori, 1996, Sec 2.3):

Let $h(\boldsymbol{x}) = \theta$ be the output and $\boldsymbol{x} \in \mathbb{R}^5$ the state defined by $\boldsymbol{x} = [\theta \ \omega \ i_1 \ i_2 \ i_3]^{\mathrm{T}}$. The system model can be put in the form $\dot{\boldsymbol{x}} = \boldsymbol{f}(\boldsymbol{x}) + \boldsymbol{g}(\boldsymbol{x})\boldsymbol{u}$, with

$$\boldsymbol{f}(\boldsymbol{x}) = \begin{bmatrix} \omega \\ \frac{1}{J}\big(-k_{\mathrm{m}}\boldsymbol{E}^T(\theta)\boldsymbol{i}\big) \\ \boldsymbol{D}^{-1}\big(k_{\mathrm{e}}\omega\boldsymbol{E}(\theta) - \boldsymbol{R}\boldsymbol{i}\big) \end{bmatrix} \tag{6}$$

$$\boldsymbol{g}(\boldsymbol{x}) = \frac{1}{L+M}\begin{bmatrix} 0 & 0 & 0 \\ 0 & 0 & 0 \\ 1 & 0 & 0 \\ 0 & 1 & 0 \\ 0 & 0 & 1 \end{bmatrix}. \tag{7}$$

From these vector fields, one can construct the co–distribution associated with the observation space

$$\Omega_o = \begin{bmatrix} \mathrm{d}h \\ \mathrm{d}L_f h \\ \mathrm{d}L_f^2 h \\ \mathrm{d}L_f^3 h \\ \mathrm{d}L_f^4 h \end{bmatrix}, \tag{8}$$

where $L_f h$ denotes the Lie derivative of h with respect to the vector field $\boldsymbol{f}$ and $L_f^n h$ denotes the n-th order Lie derivative. In this case, Ω_o is a 5×5 matrix with rank 4. In fact, by examining the determinant of this matrix, it can be seen that it is not full rank unless the phase resistances, i.e. the elements of the diagonal in $\boldsymbol{R}$ are all different, which is not the case in most brushless DC motors. Furthermore, by including higher-order Lie derivatives in the co–distribution does not make Ω_o full-rank. In turn, it is very difficult to examine all the possible combinations of Lie derivatives of the vector fields $\boldsymbol{f}$ and $\boldsymbol{g}$, e.g. $\mathrm{d}L_f L_g L_f h$.

One natural step at this point is to investigate if the system is uniformly observable, i.e. if the observability depends on the input $\boldsymbol{u}$. To examine this case, we employ the method used first in Ibarra-Rojas et al. (2004). The method consists, in general terms, in comparing the states of two identical systems, with identical inputs and outputs, but starting from different initial conditions. Then one search for the solutions that satisfy the implicit differential equation. Those solutions are called *indistinguishable trajectories* and if one can define an input that satisfies such solutions, that input is called a *bad input*. For the model (2a)-(2c), the two identical systems are

$$\frac{d\theta_j}{dt} = \omega_j \tag{9a}$$

$$\frac{d\omega_j}{dt} = \frac{1}{J}\big(-k_{\mathrm{m}}\boldsymbol{E}^T(\theta_j)\boldsymbol{i}_j\big) \tag{9b}$$

$$\frac{d\boldsymbol{i}_j}{dt} = \boldsymbol{D}^{-1}\big(k_{\mathrm{e}}\omega_j\boldsymbol{E}(\theta_j) - \boldsymbol{R}\boldsymbol{i}_j + \boldsymbol{u}_j\big), \tag{9c}$$

with $j = \mathrm{a}, \mathrm{b}$. From the method it must be $\theta_{\mathrm{a}} \equiv \theta_{\mathrm{b}}$ and $\boldsymbol{u}_{\mathrm{a}} \equiv \boldsymbol{u}_{\mathrm{b}}$. Therefore, by subtracting systems a and b, one obtains

$$0 = \omega_{\mathrm{a}} - \omega_{\mathrm{b}} \tag{10a}$$

$$\frac{d\omega_{\mathrm{a}}}{dt} - \frac{d\omega_{\mathrm{b}}}{dt} = \frac{1}{J}\big(-k_{\mathrm{m}}\boldsymbol{E}^T(\theta_j)(\boldsymbol{i}_{\mathrm{a}} - \boldsymbol{i}_{\mathrm{b}})\big) \tag{10b}$$

$$\frac{d\boldsymbol{i}_{\mathrm{a}}}{dt} - \frac{d\boldsymbol{i}_{\mathrm{b}}}{dt} = \boldsymbol{D}^{-1}\big(k_{\mathrm{e}}(\omega_{\mathrm{a}} - \omega_{\mathrm{b}})\boldsymbol{E}(\theta_j) - \boldsymbol{R}(\boldsymbol{i}_{\mathrm{a}} - \boldsymbol{i}_{\mathrm{b}})\big). \tag{10c}$$

From the above equations, the solution that satisfy the stated conditions is given by

$$\boldsymbol{E}^T(\theta_j)(\boldsymbol{i}_{\mathrm{a}} - \boldsymbol{i}_{\mathrm{b}}) = 0 \tag{11a}$$

$$\boldsymbol{D}\left(\frac{d\boldsymbol{i}_{\mathrm{a}}}{dt} - \frac{d\boldsymbol{i}_{\mathrm{b}}}{dt}\right) + \boldsymbol{R}(\boldsymbol{i}_{\mathrm{a}} - \boldsymbol{i}_{\mathrm{b}}) = \boldsymbol{0}. \tag{11b}$$

Therefore, it can be concluded that there are solutions different from the trivial solution, but they do not depend on the input, and thus the system is at least uniformly detectable. Furthermore, these solutions decay exponentially to zero, since $\boldsymbol{D}$ and $\boldsymbol{R}$ are positive definite matrices. The fact that the system is uniformly detectable can be corroborated locally by employing the Hautus lemma (Sontag, 2013, Sec 7.1) as follows: Let $\boldsymbol{A} = \partial \boldsymbol{f}(\boldsymbol{x})/\partial \boldsymbol{x}|_{\boldsymbol{x}=0}$. It can be checked, by employing a symbolic computation software (*Wolfram Mathematica*) that $\lambda = 0$ is an eigenvalue of $\boldsymbol{A}$. Therefore by checking the rank of the matrix

$$\begin{bmatrix} \lambda \boldsymbol{I} - \boldsymbol{A} \\ \boldsymbol{C} \end{bmatrix} = \begin{bmatrix} -\boldsymbol{A} \\ \boldsymbol{C} \end{bmatrix}, \tag{12}$$

which is 5, the local detectability of the nonlinear system (2a)-(2c) with θ as the only output is established.

4. PROPOSED METHOD

As already mentioned in the introduction, the HRC fault effects can be detected by monitoring the stator currents and speed. The first part of the fault detection scheme design is to propose an observer to obtain an estimate of the stator currents and speed. The estimated variables are obtained from a Luenberger type observer of the form, with θ the measured variable:

$$\dot{\hat{x}}_1 = \hat{x}_2 + K_1 \tilde{x}_1 \tag{13a}$$

$$\dot{\hat{x}}_2 = -\frac{k_{\mathrm{m}}}{J} \boldsymbol{E}^T(x_1)\tilde{\boldsymbol{x}}_3 + \tau_p + K_2 \tilde{x}_1 \tag{13b}$$

$$\dot{\hat{\boldsymbol{x}}}_3 = -D^{-1}(k_{\mathrm{e}} \tilde{x}_2 \boldsymbol{E}^T - R\tilde{\boldsymbol{x}}_3 + \boldsymbol{u}) + K_3 \tilde{x}_1 \tag{13c}$$

where $\hat{x}_1 = \hat{\theta}$, $\hat{x}_2 = \hat{\omega}$, $\hat{\boldsymbol{x}}_3 = \hat{\boldsymbol{i}}$, the estimation error is $\tilde{x}_1 = x_1 - \hat{x}_1$ and the observer gains are K_1, K_2, K_3. The second part of fault detection method design is to define the residuals which are the comparison between the measured and the estimated variables.

$$r_1 = i_1 - \hat{x}_{31} \tag{14a}$$

$$r_2 = i_2 - \hat{x}_{32} \tag{14b}$$

$$r_3 = i_3 - \hat{x}_{33} \tag{14c}$$

$$r_\omega = \omega - \hat{x}_2 \tag{14d}$$

where $\hat{\boldsymbol{x}}_3 = [\hat{x}_{31}, \hat{x}_{32}, \hat{x}_{33}]$. The BLDC motor is in its nominal state (or *healthy* state) when the motor is operating without faults. Given the observer is designed using the *balanced* BLDC motor model in its nominal state the currents residuals are all equal ($r_1 = r_2 = r_3 = r_n$) with r_n the residual value in the nominal state. But, when an HRC fault occurs in phase j its residual will increase with respect to the nominal value ($r_j > r_n$), see Table 1. It is important to mention that this increment is proportional to the severity of the fault.

On the other hand, in the nominal state the speed residual is equal to its nominal value ($r_\omega = r_{n\omega}$). This residual also increases from its nominal value in the case of HRC fault ($r_\omega > r_{n\omega}$). But, in the case of an open phase fault the residual value is greater than the residual value in the case of HRC fault, therefore this residual can be used to identify the type of fault, see Table 1.

Table 1. Signature matrix for faulty phase identification.

Phase	**1**	**2**	**3**
$\boldsymbol{r}_1$	$> r_n$	r_n	r_n
$\boldsymbol{r}_2$	r_n	$> r_n$	r_n
$\boldsymbol{r}_3$	r_n	r_n	$> r_n$

Table 2. Signature matrix for fault identification.

Operation	**Nominal**	**Open phase fault**	**HRC fault**
$\boldsymbol{r}_\omega$	$r_{n\omega}$	$>> r_{n\omega}$	$> r_{n\omega}$

For online detection an identification of open phase fault and HRC fault it is possible to use a integral window as the one implemented in the article by De La Guerra et al. (2016).

5. SIMULATION RESULTS

In this section, a numerical validation of the fault detection method is presented. Simulations were made in *Mathworks Matlab–Simulink* using the parameters of the ME0913 BLDC motor, which can be found in Table 3.

Table 3. BLDC motor parameters.

Parameter	**Value**
Rated Voltage	120 [V]
r	2.4 [Ω]
L	9.5 [mH]
M	$3/7L$
k_e	0.4886 [V/rad/s]
k_m	0.6601 [Nm/A]
J	0.0024 [kgm^2]
b	0.000095 [N m s]

A cascade PI controller was programmed with gains $K_{pm} = 100$, $K_{im} = 300$, $K_{pe} = 0.2114$, $K_{ie} = 7759.9$ and sampling time of $T = 0.0001$ [s], the speed reference value is $\omega_d = 60$[rad/s]. The HRC fault was programmed by adding an additional resistance, r_{HRC}, in phase 2. The open phase fault was programmed by multiplying the third current phase by zero from time $t = 6$ [s] till the end of the simulation.

5.1 Nominal operation

The nominal operation states are shown in Figure 2 and the residual in this setting can be seen in Figure 3. The RMS value for the residuals under nominal operation is shown in Table 4.

https://doi.org/10.58571/CNCA.AMCA.2024.056

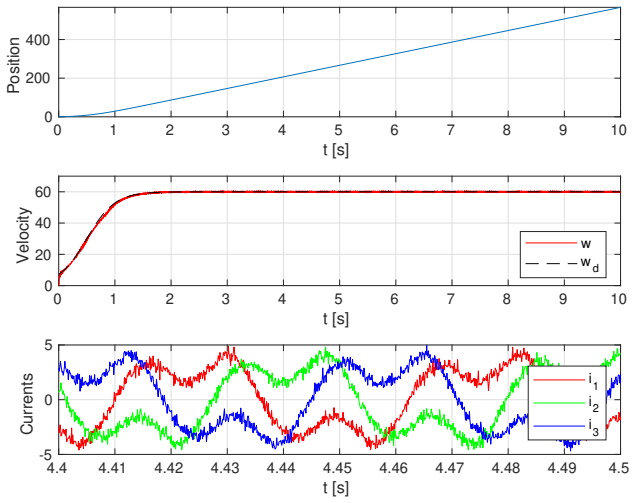

Fig. 2. BLDC states in healthy operation

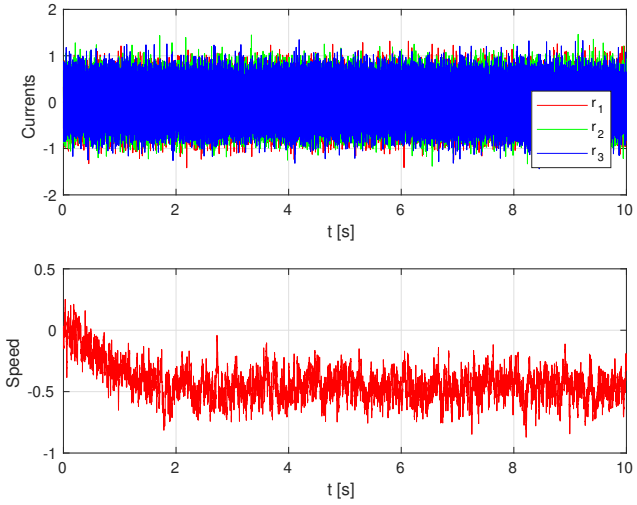

Fig. 3. Residuals in healthy operation

Table 4. RMS value for residuals in nominal operation

Phase	$\boldsymbol{r}_1$	$\boldsymbol{r}_2$	$\boldsymbol{r}_2$	r_ω
RMS	0.3213	0.3222	0.3210	0.4459

5.2 Open phase fault

The operation with an open phase fault in phase 3, that occurs in $t = 6\,[\text{s}]$, is shown in Figure 4 and the residual in this setting can be seen in Figure 5. The RMS value for the residuals under open phase operation is shown in Table 5 where all the RMS values of the residual are greater than the nominal value but it is clear that the one for the third phase has increased the most.

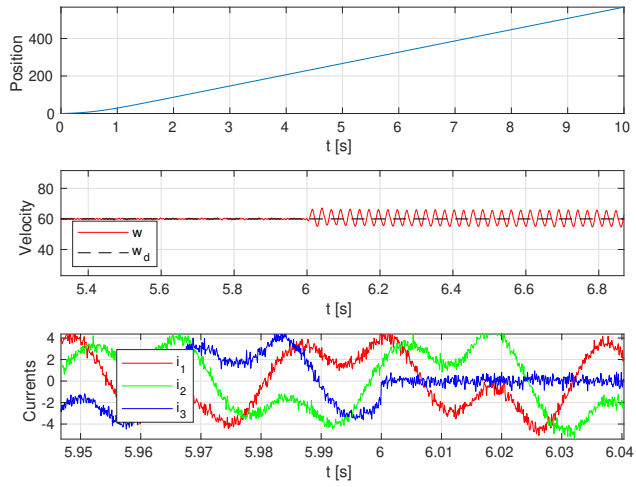

Fig. 4. BLDC states in Open phase fault

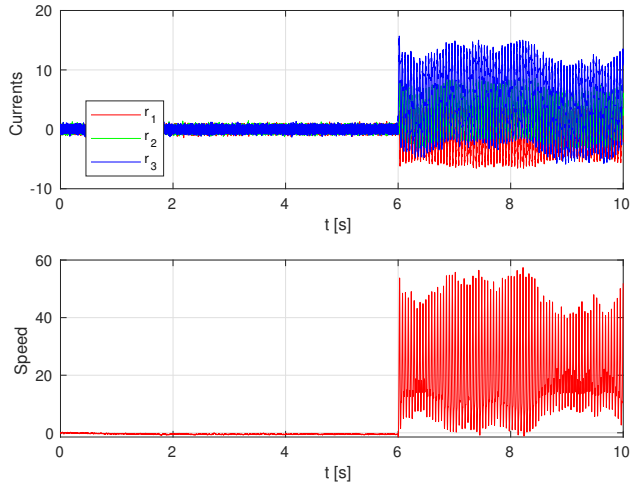

Fig. 5. Residuals with open phase fault

Table 5. RMS value for residuals in open phase fault in phase 3

Phase	$\boldsymbol{r}_1$	$\boldsymbol{r}_2$	$\boldsymbol{r}_2$	r_ω
RMS	1.7969	2.3097	**4.8002**	16.3834

5.3 High Resistance Connection fault

The operation with an HRC fault in phase 2 is shown in Figure 6 and the residual in this setting can be seen in Figure 6 and Figure 7. In particular, Figure 6 shows the residual when $r_{HRC} = 30\%r$ while Figure 7 shows the residual when $r_{HRC} = 90\%r$, comparing these Figures it is clear that the residual of the faulty phase, in green, increases as the fault resistance r_{HRC} increases. The RMS value for the residuals under HRC fault operation is shown in Table 6 where all the RMS values of the residual are greater than the nominal value but it is clear

https://doi.org/10.58571/CNCA.AMCA.2024.056

that the one for the second phase has increased the most. Moreover, the value for the residual increases as the value of the HRC resistance increases.

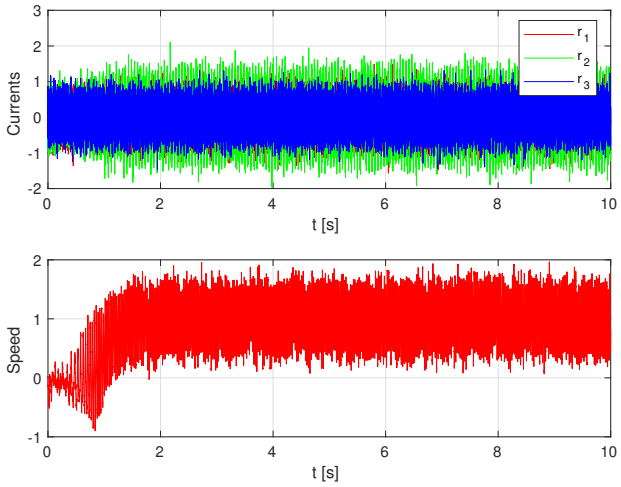

Fig. 6. Residuals with HRC fault, $r_{HRC} = 30\%r$

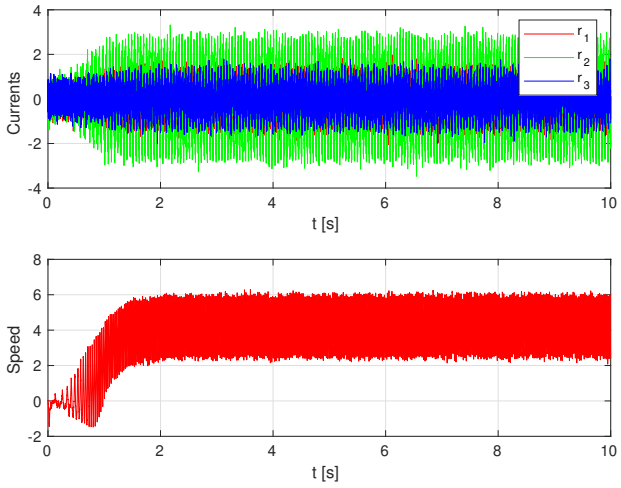

Fig. 7. Residuals with HRC fault, $r_{HRC} = 90\%r$

Table 6. RMS value for residuals in HRC fault in phase 2

r_{HRC}	r_1	r_2	r_2	r_ω
$10\%r$	0.3178	**0.3546**	0.3174	0.1905
$30\%r$	0.3376	**0.5797**	0.3300	1.0494
$45\%r$	0.3756	**0.7940**	0.3578	1.8073
$60\%r$	0.4294	**1.0162**	0.3995	2.5906
$75\%r$	0.4963	**1.2383**	0.4525	3.3922
$90\%r$	0.5714	**1.4572**	0.5139	4.2073

With respect to the fault identification, the RMS value of the speed residual is bigger for the open phase fault than for the HRC fault has can be seen by comparing Figure 6 and Figure 7. Thus, this difference in the speed residual can be used to identify the fault affecting the BLDC motor.

6. CONCLUSIONS

An identification method for HRC faults and open phase fault in Brushless DC motors is proposed in this article. An observability analysis was carried out which establishes detectability of the system when measuring only the rotor position. The numerical simulations validates the method by employing the proposed signature matrices. Although the validation is made offline, a straightforward online implementation can be made by employing a moving integral window. As future work, we will study a threshold selection methodology for fault identification. The HRC fault severity identification will be explored, and the experimental validation will be pursued as well.

REFERENCES

Chiasson, J. (2005). *Modeling and high performance control of electric machines*. John Wiley & Sons.

De La Guerra, A., Torres, L., and Maldonado-Ruelas, V. (2016). An online fault detection approach for switched reluctance motors. In *In Congreso Nacional de Control Automático 2016, Querétaro, Mexico*, 28–30.

Gupta, A., Jayaraman, K., and Reddy, R.S. (2021). Performance analysis and fault modelling of high resistance contact in brushless dc motor drive. In *IECON 2021–47th Annual Conference of the IEEE Industrial Electronics Society*, 1–6. IEEE.

Gupta, A., Reddy, R.S., and Jayaraman, K. (2024). An input current based method for fault diagnosis of high resistance connection in bldc motors. *IEEE Sensors Journal*.

Ibarra-Rojas, S., Moreno, J., and Espinosa-Pérez, G. (2004). Global observability analysis of sensorless induction motors. *Automatica*, 40(6), 1079–1085.

Isidori, A. (1996). Global almost disturbance decoupling with stability for non minimum-phase single-input single-output nonlinear systems. *Systems and Control Letters*, 28(2), 115–122.

Kudelina, K., Asad, B., Vaimann, T., Rassolkin, A., Kallaste, A., and Lukichev, D.V. (2020). Main faults and diagnostic possibilities of bldc motors. IEEE 2020 27th International Workshop on Electric Drives: MPEI Department of Electric Drives 90th Anniversary (IWED).

Sontag, E.D. (2013). *Mathematical control theory: deterministic finite dimensional systems*, volume 6. Springer Science & Business Media.

Wang, H., Qian, G., Cao, W., and Lu, S. (2022). A two-step online fault detection method for high-resistance connection faults in a vehicular bldc motor. In *Advanced Sensors and Sensing Technologies for Electric Vehicles*, 1–1. AIP Publishing LLC Melville, New York.

Yun, J., Cho, J., Lee, S.B., and Yoo, J.Y. (2009). Online detection of high-resistance connections in the incoming electrical circuit for induction motors. *IEEE Transactions on Industry Applications*, 45(2), 694–702.

